



# Speed-up, slowdown, and redirection of ice flow on neighbouring ice streams in the Pope, Smith, and Kohler region of West Antarctica

Heather L. Selley<sup>1</sup>, Anna E. Hogg<sup>1</sup>, Benjamin J. Davison<sup>1</sup>, Pierre Dutrieux<sup>2</sup>, and Thomas Slater<sup>3</sup>

<sup>1</sup>School of Earth and Environment, University of Leeds, Leeds, UK

<sup>2</sup>British Antarctic Survey, Cambridge, UK

<sup>3</sup>Department of Geography and Environmental Sciences, Centre for Polar Observation and Modelling, Northumbria University, Newcastle-Upon-Tyne NE1 8ST, UK

**Correspondence:** Heather L. Selley (h.l.selley@leeds.ac.uk)

Received: 15 May 2024 – Discussion started: 31 May 2024

Revised: 6 December 2024 – Accepted: 11 December 2024 – Published: 8 May 2025

**Abstract.** The ice streams feeding the Dotson and Crosson ice shelves are some of the fastest changing in West Antarctica. We use satellite observations to measure the change in ice speed and flow direction on eight ice streams in the Pope, Smith, and Kohler region of West Antarctica from 2005 to 2022. Seven ice streams have sped up at the grounding line, with the largest increase in ice speed at Smith West Glacier (87%), whilst Kohler West Glacier has slowed by 10%. We observe progressive redirection of ice flowlines from Kohler West into the more rapidly thinning and accelerating Kohler East Glacier, resulting in the deceleration of Kohler West Glacier and eastward migration of the ice divide between Dotson and Crosson ice shelves. These observations reveal previously undocumented impacts of spatially varying ice speed and thickness changes on flow direction and ice flux into downstream ice shelves, which may influence ice shelf and ice sheet mass change during the 21st century.

## 1 Introduction

Ice loss from Antarctica is dominated by increased grounding line discharge from ice streams draining into the Amundsen Sea Embayment (ASE) from the West Antarctic Ice Sheet (WAIS) (Joughin et al., 2010; Rignot et al., 2008, 2019; Shepherd et al., 2012, 2018). Combined, the ice streams in the ASE – Pine Island, Thwaites, Haynes, Pope, Smith, and Kohler glaciers – contain 1.2 m of sea level rise potential (Morlighem et al., 2011; Mouginot et al., 2014), and they are theoretically susceptible to marine ice sheet in-

stability (MISI) due to being grounded on predominantly retrograde bed topography (Favier et al., 2014; Joughin et al., 2014; Schoof, 2007; Weertman, 1974). MISI is theorised to occur on marine ice sheets and is an instability where the ice is grounded below sea level on bedrock that slopes downward into the interior of the ice sheet. This configuration has the potential to cause rapid retreat of the grounding line and increase ice flow into the ocean (Schoof, 2007). Across the ASE, satellite observations have shown widespread grounding line retreat (Konrad et al., 2018; Milillo et al., 2022; Scheuchl et al., 2016), thinning (Konrad et al., 2017; Pritchard et al., 2012; Rignot et al., 2019; Shepherd et al., 2018), and acceleration (Mouginot et al., 2014) since at least the early 1970s. It is likely these ice dynamic changes initiated in or before the 1940s, particularly on Pine Island Glacier (Clark et al., 2024; Davies et al., 2017; Rignot et al., 2014; Shepherd et al., 2019; Smith et al., 2016). While ice losses from Pine Island and Thwaites glaciers dominate the overall mass balance of the ASE, observations show that 21st century rates of thinning and acceleration at Pope, Smith, and Kohler (PSK) ice streams have so far been proportionally faster and higher than those of their neighbours (Davison et al., 2023; Konrad et al., 2017; McMillan et al., 2014; Mouginot et al., 2014; Rignot et al., 2014; Surawy-Stepney et al., 2023b). Ice speed and grounding line discharge at Pope, Smith, and Kohler East glaciers (Fig. 1) more than doubled between the 1970s and 2010 (Mouginot et al., 2014; Rignot et al., 2016). Smith Glacier thinned by up to  $9 \text{ m yr}^{-1}$  between 2010 and 2013 (McMillan et al., 2014), and its grounding line has retreated at speeds

of up to  $2 \text{ km yr}^{-1}$  (Konrad et al., 2018) – the fastest rate recorded in Antarctica during the satellite era.

The PSK region contains eight distinct ice streams, two of which have dual branches extending  $\sim 100 \text{ km}$  inland (Fig. 1). Haynes, Vane, Pope, Smith East, Smith West, and Kohler East glaciers flow into Crosson Ice Shelf, whereas Kohler West and Horrall glaciers flow into Dotson Ice Shelf (Fig. 1). Parts of Crosson Ice Shelf have doubled in speed, comparable to the grounded upstream areas that now flow at speeds of  $\sim 1.2 \text{ km yr}^{-1}$ , and the ice shelf has extensive rifting, particularly on its eastern side (Lilien et al., 2018; Mouginito et al., 2014) (Fig. 1). Both Dotson and Crosson ice shelves have thinned (Pritchard et al., 2012) by 10 % and 18 % (Paolo et al., 2015) between 1994 and 2012, with average basal melt rates of  $5.4 \pm 1.6$  and  $7.8 \pm 1.8 \text{ m yr}^{-1}$  between 1994 and 2018 (Adusumilli et al., 2020), respectively. Kohler West Glacier, which flows into Dotson Ice Shelf, has changed less over the last 30 years, attributed to its prograde bed slope (Milillo et al., 2022; Scheuchl et al., 2016). Satellite observations show that the grounding line of Kohler West Glacier has retreated  $200 \text{ m yr}^{-1}$  between 1992 and 2011 (Milillo et al., 2022), with no change in ice speed observed up to 2015 (Scheuchl et al., 2016) despite the ice shelf thinning near the grounding line (Gourmelen et al., 2017; Zinck et al., 2023). Despite the importance of the PSK region, due to its contemporary and potential contribution to sea level rise, the spatial pattern of its speed change since 2015 is not well characterised, and the consequences for coupled ice-shelf–ice-sheet dynamics are not adequately understood.

In this study, we combine new high-resolution satellite observations with existing measurements of ice velocity from PSK for 17.5 years from 2005–2022 to extend the record of ice speed and investigate the impact of spatially varying acceleration and thinning on ice flow direction and ice flux into Crosson and Dotson ice shelves. We measure the calving front location on Dotson and Crosson ice shelves from 2005 to 2020 to examine the impact of ice sheet velocity change on these two important Antarctic ice shelves.

## 2 Method

### 2.1 Ice velocity measurements

We measured the ice speed of Haynes, Vane, Pope, Smith, Kohler, and Horrall glaciers from January 2015 to December 2022 using Sentinel-1a and -1b synthetic aperture radar (SAR) satellite imagery (Table S2 in the Supplement). Ice velocity was measured using the intensity feature-tracking technique, which measures the displacement of visible features at or near to the ice surface such as crevasses or rifts and stable amplitude variations (Selley et al., 2021; Strozzini et al., 2002; Surawy-Stepney et al., 2023a; Wallis et al., 2023). Feature tracking was performed using the GAMMA software, with a window and step size of three (window sizes of

$256 \times 64$ ,  $362 \times 144$ , and  $400 \times 160$  for range and azimuth pixels), each with a step size of approximately 25 % of the window size, after image co-registration using precise (5 cm error) orbit ephemerides and a  $1 \times 1 \text{ km}$  digital elevation model (DEM) (Bamber et al., 2009). Errors in the velocity measurements are caused by errors in the auxiliary DEM, imprecise co-registration of the SAR images, uncertainty in locating the cross-correlation peak, and atmospheric delay due to variations in tropospheric water vapour and signal propagation speeds in the ionosphere (Hogg et al., 2017; Nagler et al., 2015). We produce a spatially varying error estimate for each image pair by dividing the ice speed by the signal-to-noise ratio of the cross-correlation function for each pixel (Lemos et al., 2018). The largest errors ( $> 30 \%$ ) occur at the rapidly deforming and highly crevassed shear margins and near each ice front; however, the centre of the major ice streams typically have a lower relative error (Fig. S2).

For each image pair, we generate a mean velocity field of all available cross-correlation window sizes that is weighted by the signal-to-noise ratio after removing outliers in the 2-D velocity fields. To remove outliers in the velocity field generated using each window size, we first compare each speed field to the nearest MEASUREs reference speed map (Mouginito et al., 2019); speed estimates more than 4 times greater or 4 times smaller than the reference map are considered outliers and are removed. Secondly, we removed velocity estimates with a signal-to-noise ratio (SNR) of less than 5.8 (De Lange et al., 2007). Third, flow directions more than  $45^\circ$  different from the reference map are considered outliers and are removed. Finally, we use a hybrid median filter with a  $3 \times 3$  moving window, which replaces central pixels with the median of the central pixel, horizontally and vertically connected pixels, and diagonally connected pixels. Hybrid median filtering is designed to remove salt and pepper noise whilst preserving edges more effectively than a traditional kernel-based median filter. We generate  $100 \times 100 \text{ m}$  annual ice speed and ice speed error maps, from 2015 to 2022, by mosaicking and averaging the image-pair speed and speed error estimates in each calendar year, in which each image pair is weighted by its SNR. Prior to annually averaging, we remove temporal outliers from the time series in two stages. First, we remove pixels that are more than five scaled median absolute deviations (MADs) from the time-series median; we then repeat this filter with a threshold of two. Secondly, we remove local time-series outliers, defined as speed estimates more than three scaled MADs from the local median in a 7-pixel moving window (approximately 6 weeks). After forming each annual mosaic, we further remove spatial outliers in two stages. First, we remove spatially isolated pixel groups, defined as contiguous regions of fewer than 100 pixels. Secondly, we remove pixels with unrealistically rapid changes in flow direction and speed, defined as pixels in which the flow direction differs by more than  $35^\circ$  or the speed differs by more than two standard deviations from the median of the surrounding pixels in a  $5 \times 5$  kernel. Finally,

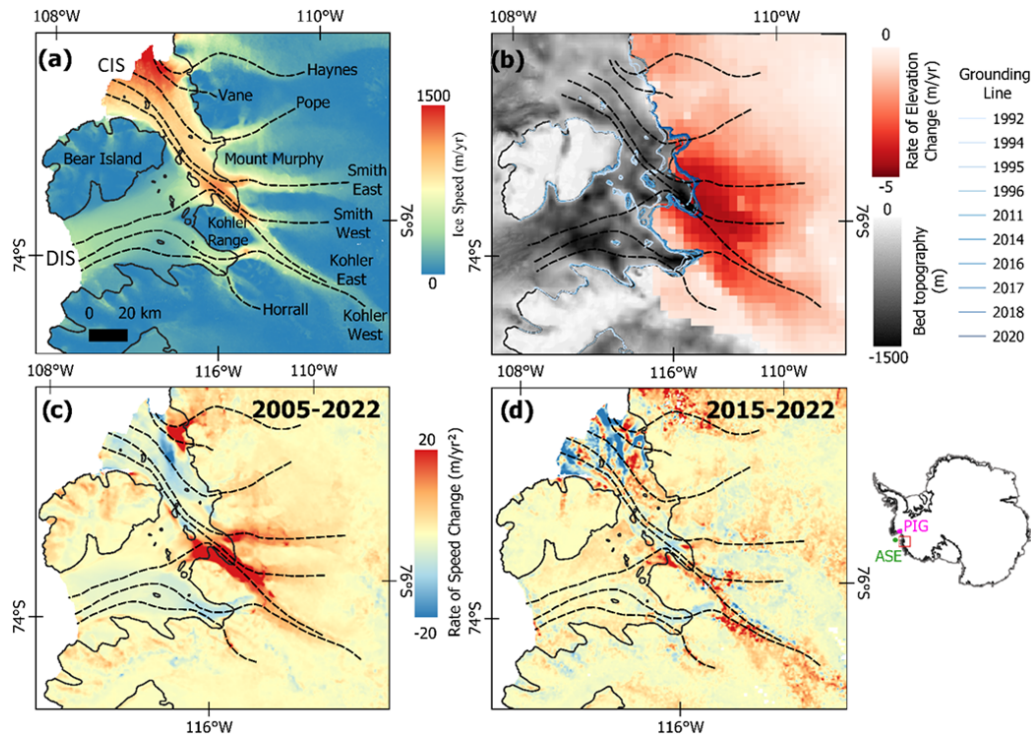


**Figure 1.** Ice speed and rate of speed change at Haynes, Vane, Pope, Smith East, Smith West, Kohler East, Kohler West, and Horrall glaciers, which feed Crosson Ice Shelf (CIS) and Dotson Ice Shelf (DIS) in the Amundsen Sea sector of West Antarctica. (a) Sentinel-1 SAR-derived average speed (2015–2022). The 2011 grounding line location (solid black line) (Rignot et al., 2016) and the location of the eight flowline profiles (dashed black lines) are also shown. (b) Rate of elevation change for 1992 to 2023 (red) (Shepherd et al., 2019) and grounding line locations from 1992 to 2020 (blue) are shown (Milillo et al., 2022; Rignot et al., 2016). (c) Observed rate of speed change over the full 17.5-year study period, from 1 May 2005 to 30 May 2022. (d) Observed rate of speed change during the Sentinel-1 period from 1 June 2015 to 31 May 2022. Measurements are superimposed on the BedMachine bedrock topography (Morlighem et al., 2017).

we perform a second filter based on eight-directional speed gradients, where small ( $< 1 \text{ km}^2$ ) regions enclosed by large speed gradients (more than  $50 \text{ m yr}^{-1}$  over  $100 \text{ m}$  (1 pixel)) are removed.

We used the MEaSURES  $1 \times 1 \text{ km}$  Antarctic annual ice velocity data (Mouginot et al., 2017) to calculate the longer-term rate of ice speed change from 2005. This dataset was generated from a combination of SAR and optical imagery acquired over the period of 1 June 2005 to 31 May 2017, using both intensity-tracking and interferometric techniques (Mouginot et al., 2017) (Tables S2 and S3). Combined with our new speed measurements, this study presents a 17.5-year-long record of ice speed measurements from June 2005 to December 2022 (Fig. S2). For time-series analysis, we extract ice speed measurements along flowline transects located on the fast-flowing central trunk of all eight ice streams (Figs. 1a and 2) and compute grounding-zone time-series averaging within  $2.5 \text{ km}$  diameter circles where the flowlines intersect with the grounding line (Rignot et al., 2016). To explore the shorter-term (sub-decadal) variability, data were detrended by subtracting the linear trend. To establish how the change in flow direction impacts the ice flux into the ice

shelves, the upstream flux was calculated by seeding flowlines from the calving front in 2005 and 2019; then it was calculated at every  $100 \text{ m}$  along each flowline. The flux was then integrated along each flowline and gridded for plotting and differencing. Velocity vectors were rotated parallel to the flowline to capture the mass flux every  $100 \text{ m}$ . A static thickness (Fretwell et al., 2013) was used to explore purely the impact of ice speed and flow direction changes.

## 2.2 Change in calving front location and ice shelf rifts

We measured the annual calving front location of the Crosson and Dotson ice shelves from 2005 to 2022 using Moderate Resolution Imaging Spectroradiometer (MODIS) imagery (Andreasen et al., 2023). Images were acquired from mid-January to the end of February to ensure consistent temporal sampling, to use relatively cloud-free data, and to avoid aliasing seasonal variation. The calving fronts were manually delineated (Cook et al., 2005; Cook and Vaughan, 2010), and the annual resolution allows for an overview of the calving front changes on the 17.5-year timescale. The uncertainty of the calving front location measurement is limited by the accuracy with which the boundary can be delineated

and the accuracy of the image georeferencing. Annual ice shelf area measurements were calculated by using the annual calving fronts to modify a reference ice shelf mask (Rignot et al., 2011). To quantify any changes in Crosson Ice Shelf, we measured the area where the calving front location extends inland of the compressive arch location from Lilien et al. (2018), assuming that the arch position is static throughout our study period. We also manually delineated a persistent, long ( $\sim 12$  km) ice shelf rift near Bear Peninsula using the Sentinel-1 amplitude images and calculated the distance between the rift tip's end and Bear Island's easternmost point.

### 3 Results

#### 3.1 Ice velocity

Our ice speed measurements show that, of the eight major ice streams in the PSK region, six ice streams reached mean speeds of over  $700 \text{ m yr}^{-1}$  in 2022, with the fastest-flowing regions of the ice streams extending up to 75 km inland of the grounding line (Fig. 1a). The fastest flowing ice streams are in the centre of the PSK region, where Kohler East, Smith West, and Smith East glaciers flow at speeds up to  $1215 \pm 275 \text{ m yr}^{-1}$  in 2022 (Table 1, Fig. 2). Relatively slower-moving ice is transported to the west of the inland Kohler Range through Kohler West and Horrall glaciers, which flow at speeds of  $715 \pm 319$  and  $401 \pm 173 \text{ m yr}^{-1}$  at the grounding line in 2022, respectively. Ice is discharged through Pope, Vane, and Haynes glaciers which flow at speeds of  $772 \pm 211$ ,  $203 \pm 93$ , and  $810 \pm 169 \text{ m yr}^{-1}$  in 2022, respectively (Table 1).

#### 3.2 Change in ice speed

We used our ice velocity measurements to fit a linear trend for each pixel to calculate the rate of change in ice speed from all speed data (MEASUREs and Sentinel-1) (2005 to 2022) and for the Sentinel-1 period (2015–2022) across the PSK region (Fig. 1b and c). We exclude pixels with fewer than five annual velocity estimates and retain speed change estimates where the fit was significant ( $p < 0.05$ ) (Selley et al., 2021). Our results show that seven ice streams in the study region have sped up since 2005, with four of those ice streams speeding up by over 60% at the grounding line (Table 1). We observe the largest percentage increase in ice speed at the grounding zone of Smith West Glacier, where the rate of ice flow increased by 87% over the 17.5-year study period, reaching speeds of  $1.2 \text{ km yr}^{-1}$  by 2022 (Fig. 3a and Table 1). The fastest absolute rate of speed change was observed on Kohler East and Smith West glaciers where ice speeds increased by  $32 \text{ m yr}^{-2}$  from 2005 to 2022 (Table 1). High rates of speed change are also observed on Haynes ( $17 \text{ m yr}^{-2}$ ) and Smith East ( $14 \text{ m yr}^{-2}$ ) glaciers (Table 1); the central region containing Kohler East, Smith West, and Smith East glaciers,

accounts for 74% of all the observed speed-up at the grounding line (Fig. 1).

Our results show that there is significant spatial variability in the observed speed change signal across the PSK region and that change on individual ice streams has not been linear throughout the 17.5-year study period. In the central and eastern regions of PSK, although ice flow has sped-up throughout the study period, the rate of speed-up since 2015 was lower than that observed in the preceding decade between 2005 and 2015 (Table 1). In contrast, ice flow on Kohler West Glacier was 10% slower in 2022 relative to its 2005 ice speed, with the slowdown starting around 2012. The western side of Dotson Ice Shelf into which these ice streams flow has also decelerated by  $-5 \text{ m yr}^{-2}$  since 2005 (Fig. 1a and b). On Kohler West Glacier, the rate of ice flow slowdown has increased since 2015 ( $-8 \text{ m yr}^{-2}$ ) compared to the 2005 to 2015 mean ( $-4 \text{ m yr}^{-2}$ ) (Table 1).

In addition to these long-term trends, we find that all ice streams in the PSK region exhibit clear short-term (sub-decadal) speed variability in addition to the 17.5-year trend (Fig. 3). This short-term variability is characterised by a period of rapid speed-up on all ice streams, excluding Kohler West Glacier, from 2005 to 2010 (14%) and from 2014 to 2017 (12%), albeit minimal for Horrall Glacier. These speed-up episodes were separated by periods of steady or decelerating ice flow from 2011 to 2013 ( $-4\%$ ) and from 2017 to the end of the study period in 2022 ( $-2\%$ ) (Fig. 3a). There is some variability in the timing of these speed variations across the PSK region: slow-down begins later (2013) at Vane Glacier and is more prolonged at Pope Glacier (2012–2015), whilst the overall slow-down of Kohler West Glacier also began around 2012 but was sustained throughout the remainder of the study period.

#### 3.3 Redirection of ice flow

Our ice velocity measurements reveal a substantial change in the direction of ice flow on two ice streams in the PSK study region (Figs. 4 and S1 and Table S1 in the Supplement), with three key changes in flow structure being especially notable. Firstly, at the division between Kohler West Glacier and Kohler East Glacier, we observe an eastward rotation ( $\sim 8^\circ$ ) of the ice flow vectors by 2019 (Fig. 4d). Examination of ice flowlines generated from velocity measurements further shows that this rotation results in redirection of ice flow from Kohler West Glacier into Kohler East Glacier, which we interpret as a form of “ice piracy” resulting from the differential rates of surface lowering observed at this ice stream division (Fig. 4). Secondly, we observe a westward rotation of the flow vectors ( $\sim 2^\circ$ ) in the region just downstream of the grounding lines of Kohler East and Smith West glaciers, indicative of increased routing of ice into Dotson Ice Shelf that had previously fed Crosson Ice Shelf (Fig. 4). Thirdly, the ice divide between Dotson and Crosson ice shelves has migrated eastward within the study period (Fig. 4). These

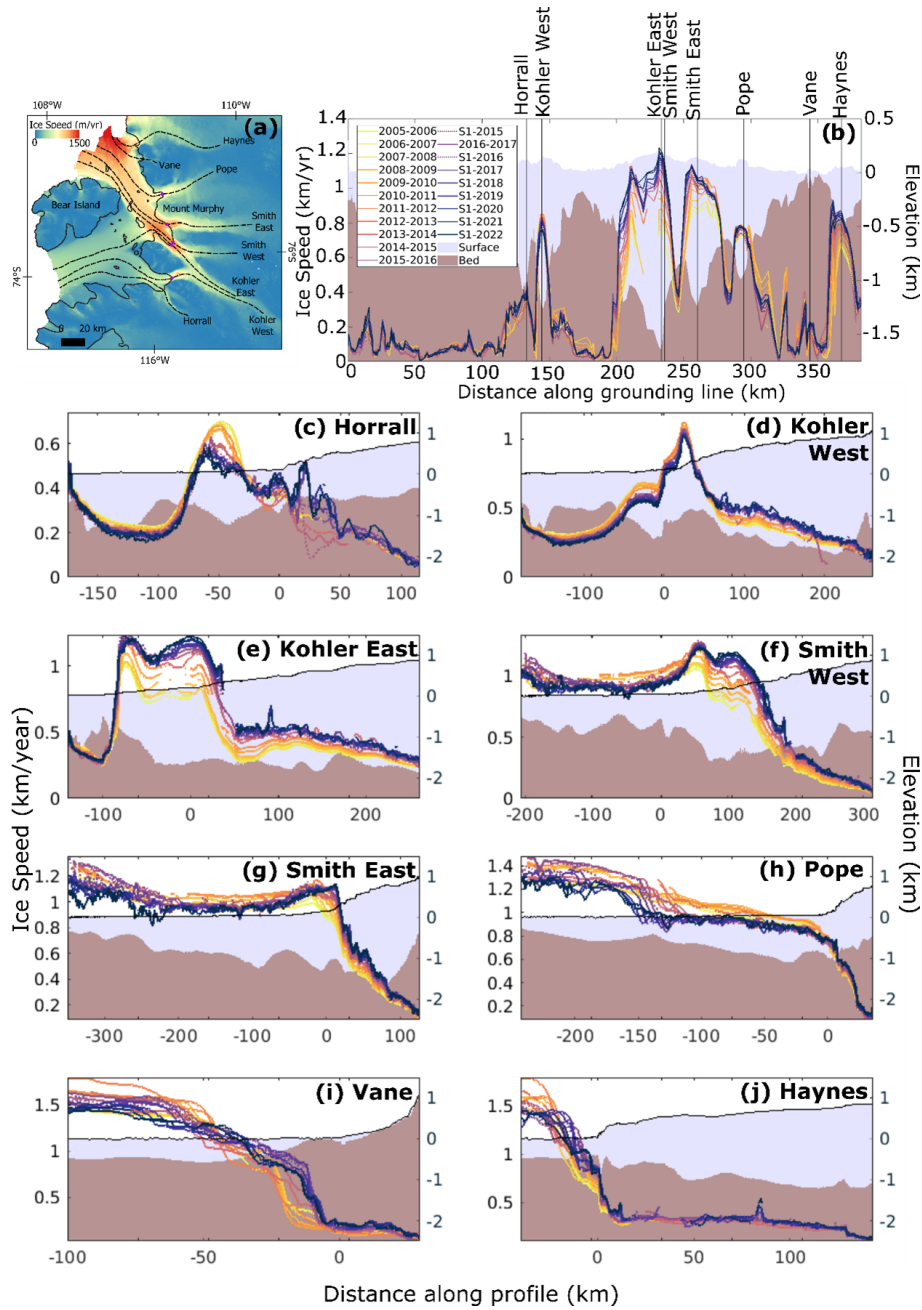


**Figure 2.** (a) Sentinel-1 SAR-derived average 2015 to 2022 ice speed over the PSK region. The 2011 grounding line location (solid black line) (Rignot et al., 2016), the location of the eight flowline profiles (dashed black lines), and the intersection 2.5 km buffer (purple circles) are also shown. (b) Observed ice speed from 2005 to 2022 at the 2011 grounding line (Rignot et al., 2016) of Dotson and Crosson ice shelves in the Amundsen Sea sector of West Antarctica. The x axis is shown as distance from the grounding line, with positive values indicating the inland section of the profile on the ice sheet and with negative values indicating seaward locations. Also shown are the intersections of flowlines (black vertical lines), the bed topography (brown shading), and ice surface elevation and thickness (grey shading) from BedMachine (Morlighem et al., 2017). Observed speed along the flowlines for (c) Horrall (d) Kohler West, (e) Kohler East, (f) Smith West, (g) Smith East, (h) Pope, (i) Vane, and (j) Haynes.

**Table 1.** The observed mean ice speed in 2022, rate of speed change during 2005–2022 and during the Sentinel-1 period (2015–2022), the percentage speed-up for both periods, and the rate of surface elevation change (1992–2023) (Shepherd et al., 2019) for the eight major ice streams in the PSK region.

Region	Ice stream name	Mean ice speed in 2022 (m yr <sup>-1</sup> )	Rate of speed change from 2005–2022 (m yr <sup>-2</sup> )	Rate of speed change for Sentinel-1 period (2015–2022) (m yr <sup>-2</sup> )	Speed change from 2005–2022 (%)	Speed change in Sentinel-1 period (2015–2022) (%)	Rate of surface elevation change (m yr <sup>-1</sup> )
Western	Horrall	401 ± 173	2	4	10	9	−0.8
	Kohler West	715 ± 319	−5	−2	−10	−3	−1.1
Central	Kohler East	1215 ± 275	32	7	84	5	−2.5
	Smith West	1188 ± 253	32	11	87	8	−2.6
	Smith East	1093 ± 416	14	0	30	0	−2.7
Eastern	Pope	772 ± 210	3	1	7	1	−2.2
	Vane	203 ± 93	5	5	76	22	−0.9
	Haynes	810 ± 169	17	10	60	11	−1.1

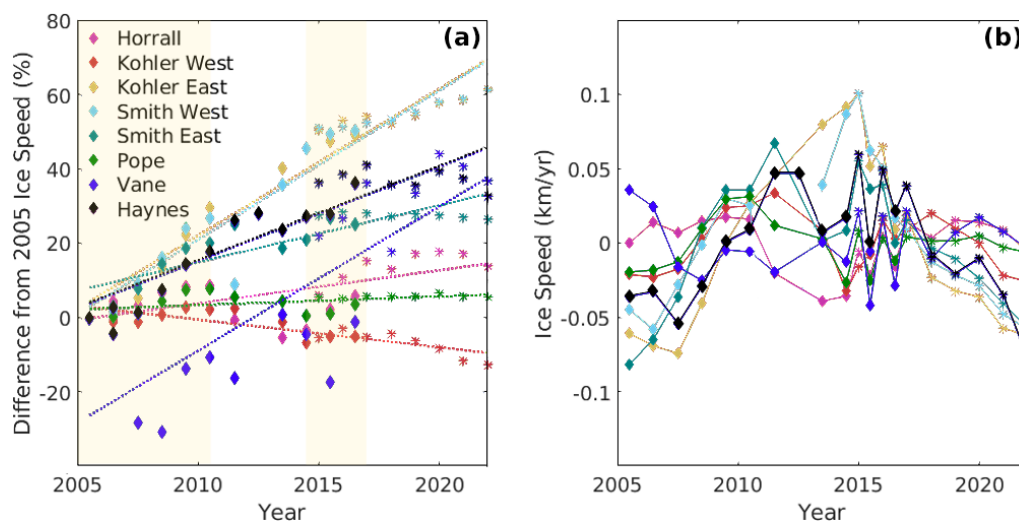


**Figure 3.** Observed relative speed change on eight major ice streams in PSK over the 15-year study period. **(a)** Percentage change in speed from 2005 to 2022, from MEaSUREs (diamonds) (Mouginot et al., 2014) and Sentinel-1 (asterisks) velocity data, calculated as the difference in speed from the 2005 measurement. All measurements were extracted from a 2.5 km diameter region where the central flowline crosses the grounding line (Fig. 1a) (Rignot et al., 2016). The shaded regions represent the rapid periods of speed-up demonstrating the periodicity around the 17.5-year trend. **(b)** Detrended annual ice speeds for each of the eight glaciers from 2005 to 2022, from MEaSUREs (diamonds) and Sentinel-1 (asterisks) velocity data, calculated as the difference in speed from the 2005 measurement. All measurements were extracted from a 2.5 km diameter region where the central flowlines (Fig. 1a) cross the grounding line (Rignot et al., 2016).

changes in flow direction have had an impact on the advection of ice from Kohler West and Kohler East into Dotson and Crosson ice shelves, resulting in increased flux into Dotson and a smaller increase in flux into Crosson than would have been the case had flow directions remained stable (Fig. 4).

### 3.4 Change in calving front location and ice shelf rift growth

Our measurements of the Dotson Ice Shelf calving front location show that the ice edge has remained in a relatively constant position throughout the study period, with a small ( $\sim 4$  km) but constant advance of its eastern limit until 2021 and a slight ( $\sim 5$  km) retreat in the west from 2005 to

2022 (Fig. 5). In contrast, the calving front of Crosson Ice Shelf has undergone several phases of retreat since 2005, the largest of which occurred in the period between 2013 and 2014. Overall, the calving front retreated by  $\sim 60$  km, losing an  $\sim 85$  km<sup>2</sup> area inland of the 1996 compressive arch (Lilien et al., 2018) at the eastern shelf edge and becoming heavily crevassed. During the same period as these large calving events, a 5 km rift formed at the eastern margin of Crosson Ice Shelf and grew to  $\sim 12$  km across the width of the ice shelf toward Bear Island during the study period (Figs. 5b, S1, and S3). The distance between the end of the rift and Bear Island decreased from 8 km in 2015 to 5 km in 2022, with the rate of rift growth slowing from 2016 to 2022. If the

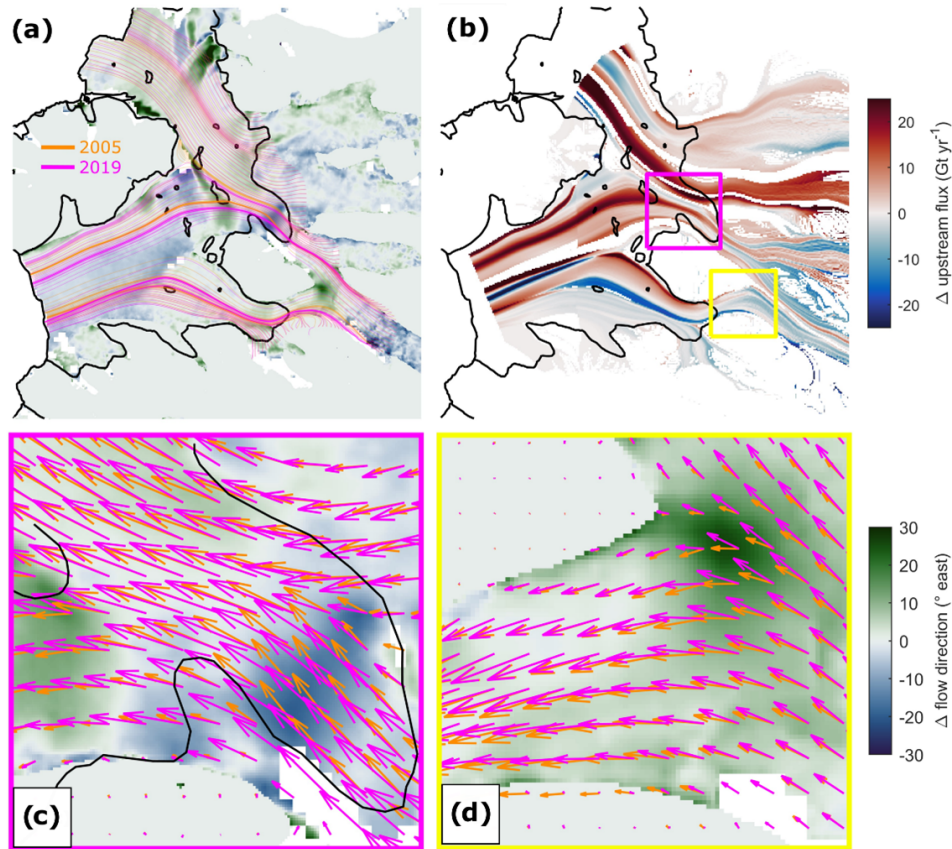


**Figure 4.** Flowlines and direction changes in the central Pope, Smith, and Kohler region. **(a)** Flowlines at the grounding line of the central PSK region for 2005 (orange) and 2019 (pink). Flow direction change (colour shading) and the grounding line location (solid black line) (Rignot et al., 2016) are also shown. **(b)** Change in upstream flux for 2019 compared to 2005 calculated and displayed cumulatively along the flowlines from inland to the calving front, which indicates where ice mass is predominantly being directed on the ice shelves. Calculated using a time-varying ice thickness drawing on elevation change observations (Shepherd et al., 2019). Panels **(c)** and **(d)** show flow direction change and flow vectors in sub-regions near **(c)** the grounding line of Kohler East Glacier and **(d)** the division between Kohler West and Kohler East.

rift eventually reaches Bear Island, an  $\sim 4 \text{ km}^2$  iceberg may be released.

After the 2014 calving event, the shape of the shelf remains convex and in a fairly consistent configuration, with smaller further-inland penetration, for example in 2016 ( $\sim 10 \text{ km}$  further). This positioning is maintained with additional fracturing and rifting gradually penetrating further across to the western side of the shelf. Notably, in 2021 there is an advance in the floating ice in front of Haynes Glacier which partially recloses the open pathway of water accessing the eastern side of Crosson Ice Shelf. In 2022, this configuration persists; however, the shear margin in front of Mount Murphy fractures and partially detaches. The substantial visible increase in damage on Crosson Ice Shelf inland of the compressive arch will have reduced the buttressing strength provided by the ice shelf, contributing to the observed speed-up of the glaciers that drain into it (Fig. 5).

#### 4 Discussion

Overall, our results extend the record and show a long-term speed-up at most major ice streams in the PSK study region from 2005 to 2022, with an average speed increase at the grounding line of 51 %. Previous work focused on the longer-term changes back to the 1970s (Mouginot et al., 2014); here we focus on the short-term changes visible from the annual records available from 2005. Although speed-up is greatest at the grounding line (Mouginot et al., 2014), it also extends up to  $\sim 100 \text{ km}$  inland (Fig. 1b, c), impacting a substantial portion of the West Antarctic Ice Sheet. The zone of highest relative speed-up is located inland of Bear Island on Smith West Glacier where the ice is thickest (Lilien et al., 2018), where the bedrock is deepest (Schoof, 2007), and where the grounding line has retreated the most (Konrad et al., 2017) (Table 1, Figs. 1b and c and 2). During their overlapping periods, our observations of speed change closely agree with previous studies in terms of the magnitude and spatial patterns of

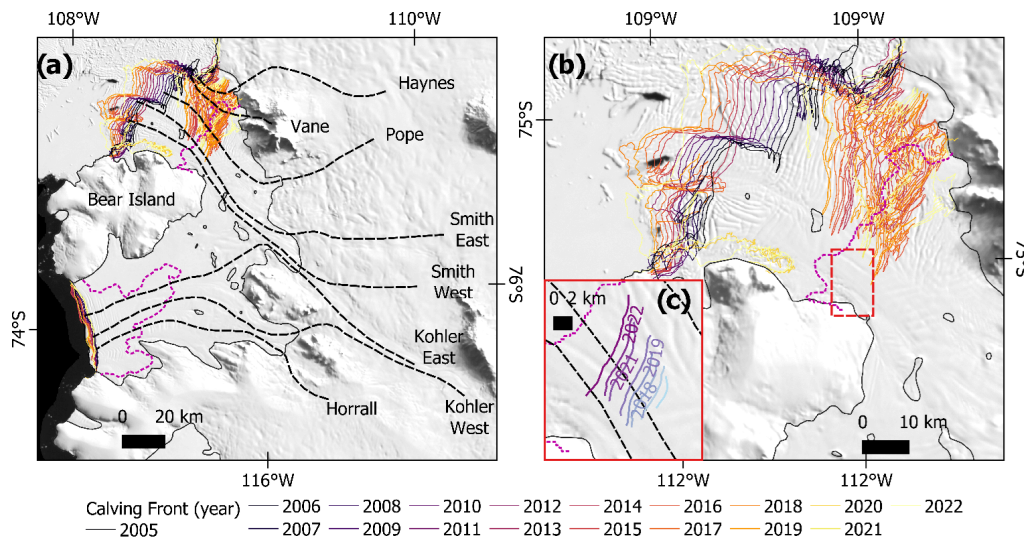


**Figure 5.** Dotson Ice Shelf and Crosson Ice Shelf calving front and rift locations. (a) Dotson Ice Shelf and Crosson Ice Shelf calving front locations from 2005 to 2022 and the compressive arches (dotted pink line) (Lilien et al., 2018) are shown superimposed on the MODIS mosaic (Scambos et al., 2007). (b) Zoomed-in view of Crosson Ice Shelf calving front locations from 2005 to 2022. (c) Location of the rift approaching Bear Island through the Sentinel-1 period (2015–2022).

speed change (Lilien et al., 2018; Miles et al., 2022; Mouginit et al., 2014; Scheuchl et al., 2016), which are consistent with observed patterns of grounding line retreat (Rignot et al., 2014) and surface elevation change (McMillan et al., 2014). Our examination of individual ice stream behaviour and our addition of more recent observations add further detail to our understanding of the evolution of the PSK region.

#### 4.1 Short-term periodicity

In addition to the long-term speed-up, we observe shorter-term ice speed variability superimposed on the long-term speed-up of most glaciers in the study region. We note periods of rapid speed-up from 2005 to 2011 with an average speed difference across all ice streams of 14 %, and during 2014–2017 (12 %) periods of speed-up were interrupted by periods of slowdown between 2011–2013 (−4 %) and 2017–2020 (−2 %) (Fig. 3a); the timing and relative magnitude of these speed fluctuations vary between ice streams, but the absolute magnitude of the speed change is similar across the region (Fig. 1). Similar ice speed variability during these periods has previously been documented at Pope Glacier, Kohler West Glacier, and Pine Island Glacier (Lilien et al., 2018; Mouginit et al., 2014; Scheuchl et al., 2016). At Pine Island Glacier, this ice speed variability is attributed to fluctuations in the depth of the thermocline on the continental shelf (Assmann et al., 2013; Dotto et al., 2019; Walker et al., 2007; Webber et al., 2017). Until 2014, the shorter-term speed variability at PSK was broadly synchronous with those observed at Pine Island Glacier, implying that the thermocline depth changes and the associated changes in oceanic heat delivery to ice shelf grounding lines during those times were

widespread in the Amundsen Sea Embayment, consistent with hydrographic surveys (Jenkins et al., 2018) and numerical ocean modelling (Naughten et al., 2022a). Pine Island Glacier has rapidly sped up since 2017 (Davison et al., 2023; Joughin et al., 2021), whereas in the PSK region rates of speed-up have slowed or ice speeds have plateaued (Fig. 3). This may reflect the increased role of calving and damage (Lhermitte et al., 2020; Surawy-Stepney et al., 2023b) on the recent speed changes observed at Pine Island Glacier (Joughin et al., 2021). Particularly, the rate of speed-up decreasing after 2020 may also be linked to the advance in the floating ice in front of Haynes Glacier which partially recloses the pathway of open water accessing the eastern side of Crosson Ice Shelf, perhaps limiting the penetration of warmer water into the cavity. A rebuttressing of Crosson Ice Shelf may have also occurred, albeit in a new configuration, with the calving front connecting to Mount Murphy as a pinning point and lowering the rate of observed speed-up. Another contributing factor could be the ungrounding and re-pinning of ice rises beneath the ice shelves. Notably, there are two rises directly downstream from Kohler East and Smith West, and should their pinning strength change, this would result in a significant speed change. Changes in ice shelf pinning can cause destabilisation by reducing the structural stability of the shelf when ice shelves are in advanced stages of thinning (Benn et al., 2022) but also by potentially initiating calving events (Arndt et al., 2018). These processes may impact the ice shelf at different times in different regions, potentially driving some of the observed speed changes (Miles and Bingham, 2024). It also remains unclear whether there is a pathway for the ocean to flow between the Crosson and

Dotson ice shelves and how this pathway has evolved historically.

#### 4.2 Kohler West slowdown

In contrast to the rest of the region, Kohler West Glacier did not speed up appreciably after 2013, resulting in a moderate ( $\sim 10\%$ ) slowdown since 2012. The lack of significant speed-up of Kohler West Glacier has been attributed to the prograde bed slope on which the grounding line rests (Milillo et al., 2022), making the ice stream less susceptible to ice dynamic change and instability. The region continues to thin; therefore, thinning-induced reductions in driving stress may have contributed to the observed slowdown. Indeed, 18 m of thinning and a  $0.03^\circ$  decrease in ice surface slope (comparable to those observed on Kohler West) would cause an  $82 \text{ m yr}^{-1}$  decrease in ice velocity, which is similar to the observed slow-down from 2005 to 2022 (Eq. S1 in the Supplement; Cuffey and Paterson, 2010). In conjunction with this deceleration of Kohler West, we observe redirection of ice flow from Kohler West Glacier into Kohler East Glacier (Fig. 4). We suggest that this so-called ice piracy results from the differential thinning rates of Kohler West (less than  $2 \text{ m yr}^{-1}$ ) and Kohler East glaciers (up to  $9 \text{ m yr}^{-1}$ ) over the last few decades (McMillan et al., 2014; Nilsson et al., 2022). These changes in flow direction are consistent with the observed changes in surface elevation and ice thickness in this region and would be expected to occur elsewhere in places where the geometry permits, such as at Totten and Vanderford glaciers (McCormack et al., 2023). Analogous historical changes in flow direction and ice divide migration have been inferred from chemical tracers (Iizuka et al., 2010) and are widely documented in paleo-ice-sheet reconstructions (Catania et al., 2012; Conway et al., 2002; Conway and Rasmussen, 2009; Iizuka et al., 2010), whilst ongoing ice divide migration has been inferred from isochrones (Nereson et al., 1998) and thickness change measurements (Conway and Rasmussen, 2009). To our knowledge, the redirection of ice flow from one ice stream to another has not been observed directly on  $\sim 15$ -year timescales, although it may have occurred at glacier or ice cap timescales. Differential thinning near ice stream boundaries is not isolated to this study region; therefore, we expect that ice divide migration and the associated changes in flow direction have and will occur elsewhere in Antarctica, and this should be considered when interpreting observed changes in ice speed and ice thickness in tightly connected regions. Modelling work indicates that minor changes in ice sheet geometry can result in ice piracy and highlights the importance of quantifying the rates of change and subsequent impact on ice mass loss (McCormack et al., 2023).

#### 4.3 Crosson and Dotson ice shelves

The observed changes in flow speed and flow direction have downstream consequences for Dotson and Crosson ice shelves. The slow-down of Kohler West Glacier has reduced the ice flux into Dotson Ice Shelf by 0.68 Gt (11 %) locally from 2011 to 2022 (Fig. 4b). However, the discharge from Kohler East Glacier into the eastern part of Dotson Ice Shelf increased by 5.6 Gt (26 %) over the same time period because of the acceleration of Kohler East Glacier and redirection of ice flow, resulting in an eastward migration of the ice divide between Dotson and Crosson ice shelves. We suggest that the divide migration between Dotson and Crosson ice shelves has been instrumental in maintaining the apparent stability of Dotson Ice Shelf, despite the slow-down of Kohler West Glacier. In contrast, Crosson Ice Shelf deteriorated substantially during our study period, characterised by rapid thinning and extensive crevassing, which we suggest has been exacerbated by the redirection of ice from Kohler East due to the ice shelf divide migration. There has been significant variability in sub-shelf melt rates in Crosson Ice Shelf spatially and temporally over the past 20 years, with melt peaking in the early 2010s (Jenkins et al., 2018). Additionally, changes to pinning points can further cause destabilisation through initiating calving events (Arndt et al., 2018) in advanced stages of thinning (Benn et al., 2022). Further work exploring the chronology of changes to stress structures on Crosson Ice Shelf would be invaluable to further establish the interplay of these driving mechanisms.

We do not observe ice piracy occurring in any of the other ice streams in the region (Fig. 4). This is likely due to their geometry which does not result in the spatial gradient of thinning that we observe at the junction of Kohler West and Kohler East glaciers.

#### 4.4 Potential implications

Some previous research has suggested that the rapid grounding line retreat and acceleration in the PSK region is indicative, if not diagnostic, of MISI (Milillo et al., 2022). At Pine Island Glacier, the rapid reduction in ice velocity in response to the cold-water intrusion in 2012 to 2013 and presumably reduced basal melt rates has been used as evidence to suggest that MISI is not underway or at least is conditional upon continued ocean forcing (Christianson et al., 2016). Recent modelling efforts suggest that the current grounding line positions in the Amundsen Sea Embayment (ASE) are stable (Hill et al., 2023). The fluctuations in speed we observe suggest that ice streams in this region are responding to changes in external forcing similarly to Pine Island Glacier and that MISI may also not be a major dynamical factor at short (sub-decadal) timescales across the PSK region. Conversely, more recent modelling work based on Pine Island Glacier indicates that irreversible grounding line retreat between the 1940s and the 1990s is an example of MISI with recent changes being

primarily driven internally (Reed et al., 2024). We observe that ice streams on prograde (Kohler West) and retrograde bed topography are responding with opposing speed change trends (Fig. 2). This indicates that bed geometry is a key control on processes driving speed changes. It is plausible that there is still an instability which could have been triggered on centennial timescales. The speed variability is indeed superimposed on a longer-term speed-up. This may be driven by a centennial trend of ocean warming on the continental shelf (Naughten et al., 2022b), likely driven by a trend in winds over the continental shelf break (Holland et al., 2019, 2022), or it could be driven by internal ice dynamic feedbacks (such as MISI) (Reed et al., 2024) or ice–ocean feedbacks, such as changes in cavity circulation due to ice shelf thinning and grounding line retreat (Bradley et al., 2022).

## 5 Conclusions

Our 17.5-year-long record of ice speed shows continued speed-up on the majority of ice streams in the Pope, Smith, and Kohler catchment of West Antarctica; slow-down on two ice streams; and previously unreported changes in flow direction and ice divide locations. We measure concentrated regions of speed-up (51 % on average) at the grounding lines of Kohler East, Smith West, and Smith East glaciers since 2005. In contrast, Kohler West slowed down by 10 % over the 17.5-year period, with most of this occurring since 2012. This is potentially due to thinning-induced reductions in driving stress. Superimposed on these speed change trends is a notable and widespread shorter-term periodicity, which is likely driven by variations in the depth of the thermocline in the ocean water on the continental shelf, comparable to that observed in the vicinity of Pine Island Glacier. In addition to these speed changes, we also observe substantial ice flow reorganisation of both grounded and floating ice. This has been characterised by (1) redirection of ice flow from Kohler West Glacier into Kohler East Glacier, which we attribute to differential thinning of the two ice streams, and by (2) migration of the ice divide between Dotson and Crosson ice shelves, which has resulted in the redirection of ice flow from Kohler East and Smith West glaciers into Dotson Ice Shelf from Crosson Ice Shelf. These changes in flow direction have substantially altered the mass flux into Dotson and Crosson ice shelves, likely playing an important role in maintaining Dotson Ice Shelf and accelerating the deterioration of Crosson Ice Shelf. This suggests that ice flow redirection is an important component of contemporary ice sheet dynamics which is required to understand the recent structural changes in Dotson and Crosson ice shelves, which may affect their future evolution. Together, these observations reveal previously undocumented interactions between the floating and grounded ice which will affect the future sea level contribution from the PSK region.

*Data availability.* The annual ice speed mosaic, rate of ice speed change, calving front, and Bear Island crack data are available at <https://doi.org/10.1594/PANGAEA.979244> (Selley and Davison, 2025). The other datasets used in this study are publicly available via the corresponding articles in this paper: grounding lines (Rignot et al., 2016, <https://doi.org/10.5067/IKBWW4RYHF1Q>, Rignot et al., 2011, and Milillo et al., 2022), ice and bedrock elevation (Shepherd et al., 2019, Morlighem et al., 2017, Bamber et al., 2009, and Fretwell et al., 2013), ice speed (Mouginot et al., 2017, and Mouginot et al., 2019), and optical imagery (Scambos et al., 2007).

*Supplement.* The supplement related to this article is available online at <https://doi.org/10.5194/tc-19-1725-2025-supplement>.

*Author contributions.* Conceptualisation: HLS, AEH. Methodology: HLS, BJD, TS. Investigation: HLS, BJD. Visualisation: HLS, BJD. Supervision: AEH. Writing (original draft): HLS. Writing (review and editing): HLS, AEH, BJD, TS, PD.

*Competing interests.* The contact author has declared that none of the authors has any competing interests.

*Disclaimer.* Publisher's note: Copernicus Publications remains neutral with regard to jurisdictional claims made in the text, published maps, institutional affiliations, or any other geographical representation in this paper. While Copernicus Publications makes every effort to include appropriate place names, the final responsibility lies with the authors.

*Acknowledgements.* This work was led by the School of Earth and Environment at the University of Leeds. The authors gratefully acknowledge the European Space Agency, the US National Aeronautics and Space Administration, the Japan Aerospace Exploration Agency, and the Canadian Space Agency for the acquisition of ERS-1, ERS-2 (C1P9925), and Sentinel-1; Landsat-8; ALOS PAL-SAR; and RADARSAT data, respectively. We acknowledge the use of datasets produced through the NASA MEASUREs programme for funding the development of long-term climate data records from satellite observations.

*Financial support.* Funding was supported by the following: European Space Agency via the ESA PolarC Ice Shelves project (grant ESA-IPL-POE-EF-cb-LE-2019-834) as part of the ESA Polar Science Cluster (Anna E. Hogg, Benjamin J. Davison), European Space Agency with the SO-ICE project (grant ESA AO/1-85 10461/20/I-NB) as part of the ESA Polar Science Cluster (Anna E. Hogg, Benjamin J. Davison), Natural Environment Research Council via the DeCAdeS project (NE/T012757/1) (Anna E. Hogg, Benjamin J. Davison, and Pierre Dutrieux), UK Earth Observation Climate Information Service (NE/X019071/1) (Anna E. Hogg, Benjamin J. Davison), and NASA through grant 80NSSC20K1158 (Pierre Dutrieux). This research has been supported by UK Re-

search and Innovation (grant no. NE/T012757/1), the European Space Agency (grant nos. ESA-IPL-POE-EF-cb-LE-2019-834 and ESA AO/1-10461/20/I- NB), the Natural Environment Research Council (grant no. NE/X019071/1 and NE/T012757/1), and NASA (grant no. 80NSSC20K1158).

*Review statement.* This paper was edited by Etienne Berthier and reviewed by Felicity McCormack and one anonymous referee.

## References

- Adusumilli, S., Fricker, H. A., Medley, B., Padman, L., and Siegfried, M. R.: Interannual variations in meltwater input to the Southern Ocean from Antarctic ice shelves, *Nat. Geosci.*, 13, 1–5, <https://doi.org/10.1038/s41561-020-0616-z>, 2020.
- Andreasen, J. R., Hogg, A. E., and Selley, H. L.: Change in Antarctic ice shelf area from 2009 to 2019, *The Cryosphere*, 17, 2059–2072, <https://doi.org/10.5194/tc-17-2059-2023>, 2023.
- Arndt, J. E., Larter, R. D., Friedl, P., Gohl, K., Höpner, K., and the Science Team of Expedition PS104: Bathymetric controls on calving processes at Pine Island Glacier, *The Cryosphere*, 12, 2039–2050, <https://doi.org/10.5194/tc-12-2039-2018>, 2018.
- Assmann, K. M., Jenkins, A., Shoosmith, D. R., Walker, D. P., Jacobs, S. S., and Nicholls, K. W.: Variability of Circumpolar Deep Water transport onto the Amundsen Sea Continental shelf through a shelf break trough, *J. Geophys. Res.-Oceans*, 118, 6603–6620, <https://doi.org/10.1002/2013JC008871>, 2013.
- Bamber, J. L., Gomez-Dans, J. L., and Griggs, J. A.: A new 1 km digital elevation model of the Antarctic derived from combined satellite radar and laser data – Part 1: Data and methods, *The Cryosphere*, 3, 101–111, <https://doi.org/10.5194/tc-3-101-2009>, 2009.
- Benn, D. I., Luckman, A., Åström, J. A., Crawford, A. J., Cornford, S. L., Bevan, S. L., Zwinger, T., Gladstone, R., Alley, K., Pettit, E., and Bassis, J.: Rapid fragmentation of Thwaites Eastern Ice Shelf, *The Cryosphere*, 16, 2545–2564, <https://doi.org/10.5194/tc-16-2545-2022>, 2022.
- Bradley, A. T., Bett, D. T., Dutrieux, P., De Rydt, J., and Holland, P. R.: The Influence of Pine Island Ice Shelf Calving on Basal Melting, *J. Geophys. Res.-Oceans*, 127, e2022JC018621, <https://doi.org/10.1029/2022JC018621>, 2022.
- Catania, G., Hulbe, C., Conway, H., Scambos, T. A., and Raymond, C. F.: Variability in the mass flux of the Ross ice streams, West Antarctica, over the last millennium, *J. Glaciol.*, 58, 741–752, <https://doi.org/10.3189/2012JOG11J219>, 2012.
- Christianson, K., Bushuk, M., Dutrieux, P., Parizek, B. R., Joughin, I. R., Alley, R. B., Shean, D. E., Abrahamsen, E. P., Anandakrishnan, S., Heywood, K. J., Kim, T. W., Lee, S. H., Nicholls, K., Stanton, T., Truffer, M., Webber, B. G. M., Jenkins, A., Jacobs, S., Bindschadler, R., and Holland, D. M.: Sensitivity of Pine Island Glacier to observed ocean forcing, *Geophys. Res. Lett.*, 43, 10817–10825, <https://doi.org/10.1002/2016GL070500>, 2016.
- Clark, R. W., Wellner, J. S., Hillenbrand, C. D., Totten, R. L., Smith, J. A., Miller, L. E., Larter, R. D., Hogan, K. A., Graham, A. G. C., Nitsche, F. O., Lehmann, A. A., Lepp, A. P., Kirkham, J. D., Fitzgerald, V. T., Garcia-Barrera, G., Ehrmann, W., and Wacker, L.: Synchronous retreat of Thwaites and Pine Island glaciers in response to external forcings in the presatellite era, *P. Natl. Acad. Sci. USA*, 121, e2211711120, <https://doi.org/10.1073/pnas.2211711120>, 2024.
- Conway, H. and Rasmussen, L. A.: Recent thinning and migration of the Western Divide, central West Antarctica, *Geophys. Res. Lett.*, 36, 12502, <https://doi.org/10.1029/2009GL038072>, 2009.
- Conway, H., Catania, G., Raymond, C. F., Gades, A. M., Scambos, T. A., and Engelhardt, H.: Switch of flow direction in an Antarctic ice stream, *Nature*, 419, 465–467, <https://doi.org/10.1038/nature01081>, 2002.
- Cook, A. J. and Vaughan, D. G.: Overview of areal changes of the ice shelves on the Antarctic Peninsula over the past 50 years, *The Cryosphere*, 4, 77–98, <https://doi.org/10.5194/tc-4-77-2010>, 2010.
- Cook, A. J., Fox, A. J., Vaughan, D. G., and Ferrigno, J. G.: Retreating glacier fronts on the Antarctic Peninsula over the past half-century, *Science*, 308, 541–544, <https://doi.org/10.1126/science.1104235>, 2005.
- Cuffey, K. M. and Paterson, W. S. B.: *The Physics of Glaciers*, Elsevier, <https://doi.org/10.1016/C2009-0-14802-X>, 2010.
- Davies, D., Bingham, R. G., Graham, A. G. C., Spagnolo, M., Dutrieux, P., Vaughan, D. G., Jenkins, A., and Nitsche, F. O.: High-resolution sub-ice-shelf seafloor records of twentieth century ungrounding and retreat of Pine Island Glacier, West Antarctica, *J. Geophys. Res.-Earth*, 122, 1698–1714, <https://doi.org/10.1002/2017JF004311>, 2017.
- Davison, B. J., Hogg, A. E., Rigby, R., Veldhuijsen, S., van Wessem, J. M., van den Broeke, M. R., Holland, P. R., Selley, H. L., and Dutrieux, P.: Sea level rise from West Antarctic mass loss significantly modified by large snowfall anomalies, *Nat. Commun.*, 14, 1–13, <https://doi.org/10.1038/s41467-023-36990-3>, 2023.
- De Lange, R., Luckman, A., and Murray, T.: Improvement of satellite radar feature tracking for ice velocity derivation by spatial frequency filtering, *IEEE T. Geosci. Remote*, 45, 2309–2318, <https://doi.org/10.1109/TGRS.2007.896615>, 2007.
- Dotto, T. S., Naveira Garabato, A. C., Bacon, S., Holland, P. R., Kimura, S., Firing, Y. L., Tsamados, M., Wåhlin, A. K., and Jenkins, A.: Wind-Driven Processes Controlling Oceanic Heat Delivery to the Amundsen Sea, Antarctica, *J. Phys. Oceanogr.*, 49, 2829–2849, <https://doi.org/10.1175/JPO-D-19-0064.1>, 2019.
- Favier, L., Durand, G., Cornford, S. L., Gudmundsson, G. H., Gagliardini, O., Gillet-Chaulet, F., Zwinger, T., Payne, A. J., and Le Brocq, A. M.: Retreat of Pine Island Glacier controlled by marine ice-sheet instability, *Nat. Clim. Chang.*, 4, 117–121, <https://doi.org/10.1038/nclimate2094>, 2014.
- Fretwell, P., Pritchard, H. D., Vaughan, D. G., Bamber, J. L., Barand, N. E., Bell, R., Bianchi, C., Bingham, R. G., Blankenship, D. D., Casassa, G., Catania, G., Callens, D., Conway, H., Cook, A. J., Corr, H. F. J., Damaske, D., Damm, V., Ferraccioli, F., Forsberg, R., Fujita, S., Gim, Y., Gogineni, P., Griggs, J. A., Hindmarsh, R. C. A., Holmlund, P., Holt, J. W., Jacobel, R. W., Jenkins, A., Jokat, W., Jordan, T., King, E. C., Kohler, J., Krabill, W., Riger-Kusk, M., Langley, K. A., Leitchenkov, G., Leuschen, C., Luyendyk, B. P., Matsuoka, K., Mouginot, J., Nitsche, F. O., Nogi, Y., Nost, O. A., Popov, S. V., Rignot, E., Rippon, D. M., Rivera, A., Roberts, J., Ross, N., Siegert, M. J., Smith, A. M., Steinhage, D., Studinger, M., Sun, B., Tinto, B. K., Welch, B. C., Wilson, D., Young, D. A., Xiangbin, C., and Zirizzotti, A.: Bedmap2: improved ice bed, surface and

- thickness datasets for Antarctica, *The Cryosphere*, 7, 375–393, <https://doi.org/10.5194/tc-7-375-2013>, 2013.
- Gourmelen, N., Goldberg, D. N., Snow, K., Henley, S. F., Bingham, R. G., Kimura, S., Hogg, A. E., Shepherd, A., Mouginot, J., Lenaerts, J. T., and Ligtenberg, S. R.: Channelized melting drives thinning under a rapidly melting Antarctic ice shelf, *Geophys. Res. Lett.*, 44, 9796–9804, 2017.
- Hill, E. A., Urruty, B., Reese, R., Garbe, J., Gagliardini, O., Durand, G., Gillet-Chaulet, F., Gudmundsson, G. H., Winkelmann, R., Chekki, M., Chandler, D., and Langebroek, P. M.: The stability of present-day Antarctic grounding lines – Part I: No indication of marine ice sheet instability in the current geometry, *The Cryosphere*, 17, 3739–3759, <https://doi.org/10.5194/tc-17-3739-2023>, 2023.
- Hogg, A. E., Shepherd, A., Cornford, S. L., Briggs, K. H., Gourmelen, N., Graham, J. A., Joughin, I., Mouginot, J., Nagler, T., Payne, A. J., Rignot, E., and Wuite, J.: Increased ice flow in Western Palmer Land linked to ocean melting, *Geophys. Res. Lett.*, 44, 4159–4167, <https://doi.org/10.1002/2016GL072110>, 2017.
- Holland, P. R., Bracegirdle, T. J., Dutrieux, P., Jenkins, A., and Steig, E. J.: West Antarctic ice loss influenced by internal climate variability and anthropogenic forcing, *Nat. Geosci.*, 12, 718–724, <https://doi.org/10.1038/s41561-019-0420-9>, 2019.
- Holland, P. R., O'Connor, G. K., Bracegirdle, T. J., Dutrieux, P., Naughten, K. A., Steig, E. J., Schneider, D. P., Jenkins, A., and Smith, J. A.: Anthropogenic and internal drivers of wind changes over the Amundsen Sea, West Antarctica, during the 20th and 21st centuries, *The Cryosphere*, 16, 5085–5105, <https://doi.org/10.5194/tc-16-5085-2022>, 2022.
- Iizuka, Y., Miura, H., Iwasaki, S., Maemoku, H., Sawagaki, T., Greve, R., Satake, H., Sasa, K., and Matsushi, Y.: Evidence of past migration of the ice divide between the Shirase and Sôya drainage basins derived from chemical characteristics of the marginal ice in the Sôya drainage basin, East Antarctica, *J. Glaciol.*, 56, 395–404, <https://doi.org/10.3189/002214310792447707>, 2010.
- Jenkins, A., Shoosmith, D., Dutrieux, P., Jacobs, S., Kim, T. W., Lee, S. H., Ha, H. K., and Stammerjohn, S.: West Antarctic Ice Sheet retreat in the Amundsen Sea driven by decadal oceanic variability, *Nat. Geosci.*, 11, 733–738, <https://doi.org/10.1038/s41561-018-0207-4>, 2018.
- Joughin, I., Smith, B. E., and Holland, D. M.: Sensitivity of 21st century sea level to ocean-induced thinning of Pine Island Glacier, Antarctica, *Geophys. Res. Lett.*, 37, L20502, <https://doi.org/10.1029/2010GL044819>, 2010.
- Joughin, I., Smith, B. E., and Medley, B.: Marine ice sheet collapse potentially under way for the thwaites glacier basin, West Antarctica, *Science*, 344, 735–738, <https://doi.org/10.1126/science.1249055>, 2014.
- Joughin, I., Shapero, D., Smith, B., Dutrieux, P., and Barham, M.: Ice-shelf retreat drives recent Pine Island Glacier speedup, *Sci. Adv.*, 7, 3080–3091, <https://doi.org/10.1126/sciadv.abg3080>, 2021.
- Konrad, H., Gilbert, L., Cornford, S. L., Payne, A., Hogg, A., Muir, A., and Shepherd, A.: Uneven onset and pace of ice-dynamical imbalance in the Amundsen Sea Embayment, West Antarctica, *Geophys. Res. Lett.*, 44, 910–918, <https://doi.org/10.1002/2016GL070733>, 2017.
- Konrad, H., Shepherd, A., Gilbert, L., Hogg, A. E., McMillan, M., Muir, A., and Slater, T.: Net retreat of Antarctic glacier grounding lines, *Nat. Geosci.*, 11, 258–262, <https://doi.org/10.1038/s41561-018-0082-z>, 2018.
- Lemos, A., Shepherd, A., McMillan, M., Hogg, A. E., Hatton, E., and Joughin, I.: Ice velocity of Jakobshavn Isbræ, Petermann Glacier, Nioghalvfjerdingsfjorden, and Zachariæ Isstrøm, 2015–2017, from Sentinel 1-a/b SAR imagery, *The Cryosphere*, 12, 2087–2097, <https://doi.org/10.5194/tc-12-2087-2018>, 2018.
- Lhermitte, S., Sun, S., Shuman, C., Wouters, B., Pattyn, F., Wuite, J., Berthier, E., and Nagler, T.: Damage accelerates ice shelf instability and mass loss in Amundsen Sea Embayment, *P. Natl. Acad. Sci. USA*, 117, 24735–24741, <https://doi.org/10.1073/pnas.1912890117>, 2020.
- Lilien, D. A., Joughin, I., Smith, B., and Shean, D. E.: Changes in flow of Crosson and Dotson ice shelves, West Antarctica, in response to elevated melt, *The Cryosphere*, 12, 1415–1431, <https://doi.org/10.5194/tc-12-1415-2018>, 2018.
- McCormack, F. S., Roberts, J. L., Kulesa, B., Aitken, A., Dow, C. F., Bird, L., Galton-Fenzi, B. K., Hochmuth, K., Jones, R. S., Mackintosh, A. N., and McArthur, K.: Assessing the potential for ice flow piracy between the Totten and Vanderford glaciers, East Antarctica, *The Cryosphere*, 17, 4549–4569, <https://doi.org/10.5194/tc-17-4549-2023>, 2023.
- McMillan, M., Shepherd, A., Sundal, A., Briggs, K., Muir, A., Ridout, A., Hogg, A., and Wingham, D.: Increased ice losses from Antarctica detected by CryoSat-2, *Geophys. Res. Lett.*, 41, 3899–3905, <https://doi.org/10.1002/2014GL060111>, 2014.
- Miles, B. W. J. and Bingham, R. G.: Progressive unanchoring of Antarctic ice shelves since 1973, *Nature*, 626, 785–791, <https://doi.org/10.1038/s41586-024-07049-0>, 2024.
- Miles, B. W. J., Stokes, C. R., Jamieson, S. S. R., Jordan, J. R., Gudmundsson, G. H., and Jenkins, A.: High spatial and temporal variability in Antarctic ice discharge linked to ice shelf buttressing and bed geometry, *Sci. Rep.*, 12, 1–14, <https://doi.org/10.1038/s41598-022-13517-2>, 2022.
- Milillo, P., Rignot, E., Rizzoli, P., Scheuchl, B., Mouginot, J., Bueso-Bello, J. L., Prats-Iraola, P., and Dini, L.: Rapid glacier retreat rates observed in West Antarctica, *Nat. Geosci.*, 15, 48–53, <https://doi.org/10.1038/s41561-021-00877-z>, 2022.
- Morlighem, M., Rignot, E., Seroussi, H., Larour, E., Ben Dhia, H., and Aubry, D.: A mass conservation approach for mapping glacier ice thickness, *Geophys. Res. Lett.*, 38, L19503, <https://doi.org/10.1029/2011GL048659>, 2011.
- Morlighem, M., Williams, C. N., Rignot, E., An, L., Arndt, J. E., Bamber, J. L., Catania, G., Chauché, N., Dowdeswell, J. A., Dorschel, B., Fenty, I., Hogan, K., Howat, I., Hubbard, A., Jakobsson, M., Jordan, T. M., Kjeldsen, K. K., Millan, R., Mayer, L., Mouginot, J., Noël, B. P. Y., O’Cofaigh, C., Palmer, S., Rysgaard, S., Seroussi, H., Siegert, M. J., Slabon, P., Straneo, F., van den Broeke, M. R., Weinrebe, W., Wood, M., and Zinglensen, K. B.: BedMachine v3: Complete Bed Topography and Ocean Bathymetry Mapping of Greenland From Multibeam Echo Sounding Combined With Mass Conservation, *Geophys. Res. Lett.*, 44, 11051–11061, <https://doi.org/10.1002/2017GL074954>, 2017.
- Mouginot, J., Rignot, E., and Scheuchl, B.: Sustained increase in ice discharge from the Amundsen Sea Embayment, West Antarc-

- tica, from 1973 to 2013, *Geophys. Res. Lett.*, 41, 1576–1584, <https://doi.org/10.1002/2013GL059069>, 2014.
- Mouginot, J., Rignot, E., Scheuchl, B., and Millan, R.: Comprehensive Annual Ice Sheet Velocity Mapping Using Landsat-8, Sentinel-1, and RADARSAT-2 Data, *Remote Sens.*, 9, 364, <https://doi.org/10.3390/rs9040364>, 2017.
- Mouginot, J., Rignot, E., and Scheuchl, B.: Continent-Wide, Interferometric SAR Phase, Mapping of Antarctic Ice Velocity, *Geophys. Res. Lett.*, 46, 9710–9718, <https://doi.org/10.1029/2019GL083826>, 2019.
- Nagler, T., Rott, H., Hetzenecker, M., Wuite, J., and Potin, P.: The Sentinel-1 Mission: New Opportunities for Ice Sheet Observations, *Remote Sens.*, 7, 9371–9389, <https://doi.org/10.3390/rs70709371>, 2015.
- Naughten, K. A., Holland, P. R., Dutrieux, P., Kimura, S., Bett, D. T., and Jenkins, A.: Simulated Twentieth-Century Ocean Warming in the Amundsen Sea, West Antarctica, *Geophys. Res. Lett.*, 49, e2021GL094566, <https://doi.org/10.1029/2021GL094566>, 2022a.
- Naughten, K. A., Holland, P. R., Dutrieux, P., Kimura, S., Bett, D. T., and Jenkins, A.: Simulated Twentieth-Century Ocean Warming in the Amundsen Sea, West Antarctica, *Geophys. Res. Lett.*, 49, e2021GL094566, <https://doi.org/10.1029/2021GL094566>, 2022b.
- Nererson, N. A., Raymond, C. F., Waddington, E. D., and Jacobel, R. W.: Migration of the Siple Dome ice divide, West Antarctica, *J. Glaciol.*, 44, 643–652, <https://doi.org/10.3189/S0022143000002148>, 1998.
- Nilsson, J., Gardner, A. S., and Paolo, F. S.: Elevation change of the Antarctic Ice Sheet: 1985 to 2020, *Earth Syst. Sci. Data*, 14, 3573–3598, <https://doi.org/10.5194/essd-14-3573-2022>, 2022.
- Paolo, F. S., Fricker, H. A., and Padman, L.: Volume loss from Antarctic ice shelves is accelerating, *Science*, 348, 327–331, <https://doi.org/10.1126/science.aaa0940>, 2015.
- Pritchard, H. D., Ligtenberg, S. R. M., Fricker, H. A., Vaughan, D. G., Van Den Broeke, M. R., and Padman, L.: Antarctic ice-sheet loss driven by basal melting of ice shelves, *Nature*, 484, 502–505, <https://doi.org/10.1038/nature10968>, 2012.
- Reed, B., Green, J., Jenkins, A., and Gudmundsson, G. H.: Recent irreversible retreat phase of Pine Island Glacier, *Nat. Clim. Chang.*, 14, 75–81, <https://doi.org/10.1038/s41558-023-01887-y>, 2024.
- Rignot, E., Bamber, J. L., Van Den Broeke, M. R., Davis, C., Li, Y., Van De Berg, W. J., and Van Meijgaard, E.: Recent Antarctic ice mass loss from radar interferometry and regional climate modelling, *Nat. Geosci.*, 1, 106–110, <https://doi.org/10.1038/ngeo102>, 2008.
- Rignot, E., Mouginot, J., and Scheuchl, B.: Antarctic grounding line mapping from differential satellite radar interferometry, *Geophys. Res. Lett.*, 38, L10504, <https://doi.org/10.1029/2011GL047109>, 2011.
- Rignot, E., Mouginot, J., Morlighem, M., Seroussi, H., and Scheuchl, B.: Widespread, rapid grounding line retreat of Pine Island, Thwaites, Smith, and Kohler glaciers, West Antarctica, from 1992 to 2011, *Geophys. Res. Lett.*, 41, 3502–3509, <https://doi.org/10.1002/2014GL060140>, 2014.
- Rignot, E., Mouginot, J., and Scheuchl, B.: MEaSURES Antarctic Grounding Line from Differential Satellite Radar Interferometry, Version 2., Boulder, Colorado USA, NASA National Snow and Ice Data Center Distributed Active Archive Center [data set], <https://doi.org/10.5067/IKBBW4RYHF1Q>, 2016.
- Rignot, E., Mouginot, J., Scheuchl, B., Van Den Broeke, M., Van Wessem, M. J., and Morlighem, M.: Four decades of Antarctic ice sheet mass balance from 1979–2017, *P. Natl. Acad. Sci. USA*, 116, 1095–1103, <https://doi.org/10.1073/pnas.1812883116>, 2019.
- Scambos, T. A., Haran, T. M., Fahnestock, M. A., Painter, T. H., and Bohlander, J.: MODIS-based Mosaic of Antarctica (MOA) data sets: Continent-wide surface morphology and snow grain size, *Remote Sens. Environ.*, 111, 242–257, 2007.
- Scheuchl, B., Mouginot, J., Rignot, E., Morlighem, M., and Khazendar, A.: Grounding line retreat of Pope, Smith, and Kohler Glaciers, West Antarctica, measured with Sentinel-1a radar interferometry data, *Geophys. Res. Lett.*, 43, 8572–8579, <https://doi.org/10.1002/2016GL069287>, 2016.
- Schoof, C.: Ice sheet grounding line dynamics: Steady states, stability, and hysteresis, *J. Geophys. Res.-Earth*, 112, F03S28, <https://doi.org/10.1029/2006JF000664>, 2007.
- Selley, H. L. and Davison, B. J.: Ice velocity time series, rate of speed change and calving fronts in the Pope, Smith and Kohler region of West Antarctica, PANGAEA [data set], <https://doi.org/10.1594/PANGAEA.979244>, 2025.
- Selley, H. L., Hogg, A. E., Cornford, S., Dutrieux, P., Shepherd, A., Wuite, J., Floricioiu, D., Kusk, A., Nagler, T., Gilbert, L., Slater, T., and Kim, T. W.: Widespread increase in dynamic imbalance in the Getz region of Antarctica from 1994 to 2018, *Nat. Commun.*, 12, 1–10, <https://doi.org/10.1038/s41467-021-21321-1>, 2021.
- Shepherd, A., Ivins, E. R., Geruo, A., Barletta, V. R., Bentley, M. J., Bettadpur, S., Briggs, K. H., Bromwich, D. H., Forsberg, R., Galin, N., Horwath, M., Jacobs, S., Joughin, I., King, M. A., Lenaerts, J. T. M., Li, J., Ligtenberg, S. R. M., Luckman, A., Luthcke, S. B., McMillan, M., Meister, R., Milne, G., Mouginot, J., Muir, A., Nicolas, J. P., Paden, J., Payne, A. J., Pritchard, H., Rignot, E., Rott, H., Sørensen, L. S., Scambos, T. A., Scheuchl, B., Schrama, E. J. O., Smith, B., Sundal, A. V., Van Angelen, J. H., Van De Berg, W. J., Van Den Broeke, M. R., Vaughan, D. G., Velicogna, I., Wahr, J., Whitehouse, P. L., Wingham, D. J., Yi, D., Young, D., and Zwally, H. J.: A reconciled estimate of ice-sheet mass balance, *Science*, 338, 1183–1189, <https://doi.org/10.1126/science.1228102>, 2012.
- Shepherd, A., Ivins, E., Rignot, E., Smith, B., Van Den Broeke, M., Velicogna, I., Whitehouse, P., Briggs, K., Joughin, I., Krinner, G., Nowicki, S., Payne, T., Scambos, T., Schlegel, N., Geruo, A., Agosta, C., Ahlstrøm, A., Babonis, G., Barletta, V., Blazquez, A., Bonin, J., Csatho, B., Cullather, R., Felikson, D., Fettweis, X., Forsberg, R., Gallee, H., Gardner, A., Gilbert, L., Groh, A., Gunter, B., Hanna, E., Harig, C., Helm, V., Horvath, A., Horwath, M., Khan, S., Kjeldsen, K. K., Konrad, H., Langen, P., Lecavalier, B., Loomis, B., Luthcke, S., McMillan, M., Melini, D., Mernild, S., Mohajerani, Y., Moore, P., Mouginot, J., Moyano, G., Muir, A., Nagler, T., Nield, G., Nilsson, J., Noel, B., Otosaka, I., Pattle, M. E., Peltier, W. R., Pie, N., Rietbroek, R., Rott, H., Sandberg-Sørensen, L., Sasgen, I., Save, H., Scheuchl, B., Schrama, E., Schröder, L., Seo, K. W., Simonsen, S., Slater, T., Spada, G., Sutterley, T., Talpe, M., Tarasov, L., Van De Berg, W. J., Van Der Wal, W., Van Wessem, M., Vishwakarma, B. D., Wiese, D., and Wouters, B.: Mass balance of

- the Antarctic Ice Sheet from 1992 to 2017, *Nature*, 558, 219–222, <https://doi.org/10.1038/s41586-018-0179-y>, 2018.
- Shepherd, A., Gilbert, L., Muir, A. S., Konrad, H., McMillan, M., Slater, T., Briggs, K. H., Sundal, A. V., Hogg, A. E., and Engdahl, M. E.: Trends in Antarctic Ice Sheet Elevation and Mass, *Geophys. Res. Lett.*, 46, 8174–8183, <https://doi.org/10.1029/2019GL082182>, 2019.
- Smith, J. A., Andersen, T. J., Shortt, M., Gaffney, A. M., Truffer, M., Stanton, T. P., Bindschadler, R., Dutriex, P., Jenkins, A., Hillenbrand, C. D., Ehrmann, W., Corr, H. F. J., Farley, N., Crowhurst, S., and Vaughan, D. G.: Sub-ice-shelf sediments record history of twentieth-century retreat of Pine Island Glacier, *Nature*, 541, 77–80, <https://doi.org/10.1038/nature20136>, 2016.
- Strozzi, T., Luckman, A., Murray, T., Wegmüller, U., and Werner, C. L.: Glacier motion estimation using SAR offset-tracking procedures, *IEEE T. Geosci. Remote*, 40, 2384–2391, <https://doi.org/10.1109/TGRS.2002.805079>, 2002.
- Surawy-Stepney, T., Hogg, A. E., Cornford, S. L., and Davison, B. J.: Episodic dynamic change linked to damage on the Thwaites Glacier Ice Tongue, *Nat. Geosci.*, 16, 37–43, <https://doi.org/10.1038/s41561-022-01097-9>, 2023a.
- Surawy-Stepney, T., Hogg, A. E., Cornford, S. L., and Hogg, D. C.: Mapping Antarctic crevasses and their evolution with deep learning applied to satellite radar imagery, *The Cryosphere*, 17, 4421–4445, <https://doi.org/10.5194/tc-17-4421-2023>, 2023b.
- Walker, D. P., Brandon, M. A., Jenkins, A., Allen, J. T., Dowdeswell, J. A., and Evans, J.: Oceanic heat transport onto the Amundsen Sea shelf through a submarine glacial trough, *Geophys. Res. Lett.*, 34, L02602, <https://doi.org/10.1029/2006GL028154>, 2007.
- Wallis, B. J., Hogg, A. E., van Wessem, J. M., Davison, B. J., and van den Broeke, M. R.: Widespread seasonal speed-up of west Antarctic Peninsula glaciers from 2014 to 2021, *Nat. Geosci.*, 16, 231–237, <https://doi.org/10.1038/s41561-023-01131-4>, 2023.
- Webber, B. G. M., Heywood, K. J., Stevens, D. P., Dutriex, P., Abrahamsen, E. P., Jenkins, A., Jacobs, S. S., Ha, H. K., Lee, S. H., and Kim, T. W.: Mechanisms driving variability in the ocean forcing of Pine Island Glacier, *Nat. Commun.*, 8, 1–8, <https://doi.org/10.1038/ncomms14507>, 2017.
- Weertman, J.: Stability of the junction of an ice sheet and an ice shelf, *J. Glaciol.*, 13, 3–11, <https://doi.org/10.1017/S0022143000023327>, 1974.
- Zinck, A.-S. P., Wouters, B., Lambert, E., and Lhermitte, S.: Unveiling spatial variability within the Dotson Melt Channel through high-resolution basal melt rates from the Reference Elevation Model of Antarctica, *The Cryosphere*, 17, 3785–3801, <https://doi.org/10.5194/tc-17-3785-2023>, 2023.